HNPS Advances in Nuclear Physics

Vol 32 (2026)

HNPS2025

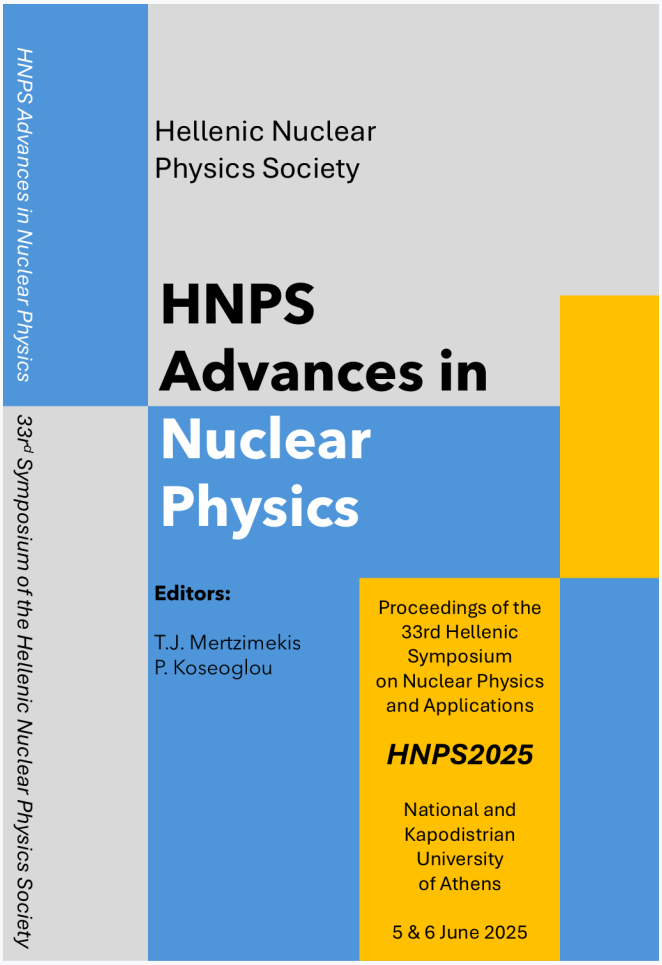

Cumulative Fission Yield Measurements from 235U(nth,f) with the FIPPS Instrument

Anna Skouloudaki, Abdelhazize Chebboubi, Maria Diakaki, Olivier Serot, Gregoire Kessedjian, Caterina Michelagnoli, Jean-Michel Daugas, Ulli Koester, Paolo Mutti, Emilio Ruiz-Martinez, Olivier Meplan

doi: 10.12681/hnpsanp.8981

To cite this article:

Skouloudaki, A., Chebboubi, A., Diakaki, M., Serot, O., Kessedjian, G., Michelagnoli, C., Daugas, J.-M., Koester, U., Mutti, P., Ruiz-Martinez, E., & Meplan, O. (2026). Cumulative Fission Yield Measurements from 235U(nth,f) with the FIPPS Instrument. *HNPS Advances in Nuclear Physics*, *32*, 212–219. https://doi.org/10.12681/hnpsanp.8981

HNPS Advances in Nuclear Physics Vol. **32**, 212–219 (2025)
doi: 10.12681/hnpsanp.8981

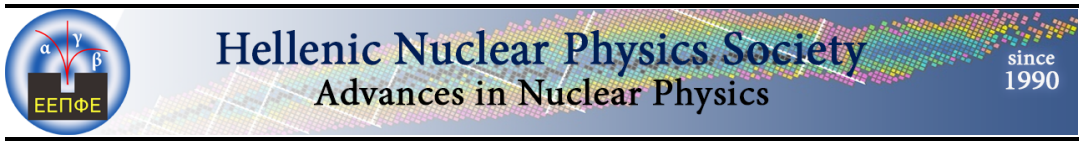

ARTICLE

Cumulative Fission Yield Measurements from ^{235}U(n_{th}, f) with the FIPPS Instrument

A. Skouloudaki,[*,1,2] A. Chebboubi,[1] M. Diakaki,[2] O. Serot,[1] G. Kessedjian,[1] C. Michelagnoli,[3] J.M. Daugas,[3] U. Köster,[3] P. Mutti,[3] E. Ruiz,[3] and O. Meplan[4]

[1]CEA, DES, IRESNE, DER, SPRC, Cadarache, Physics Studies Laboratory, 13108 Saint-Paul-lés-Durance, France
[2]National Technical University of Athens, Iroon Polytechniou 9, Zografou Campus 15780, Athens, Greece
[3]Institut Laue-Langevin, 38042 Grenoble Cedex 9, France
[4]LPSC, Université Grenoble-Alpes, CNRS/IN2P3, 38026 Grenoble Cedex, France
*Corresponding author: Anna.SKOULOUDAKI@cea.fr

(Received: 25 Nov 2025; Accepted: 14 Feb 2026; Published: 17 Feb 2026)

Abstract

This work reports high-precision cumulative yield measurements of key isotopes from ^{235}U(n_{th}, f) reactions using the FIPPS (FIssion Product Prompt γ-ray Spectrometer) at ILL, representing the first dedicated cumulative fission yield campaign in the facility.

In this work, advanced spectroscopic techniques were employed to reduce nuclear data uncertainties, while evaluating FIPPS capabilities for fission yield measurements.

A pre-irradiated ^{235}U target was exposed to a high neutron flux, and the resulting γ-rays were recorded using a 16-element HPGe Clover array. A 7-day irradiation at a thermal neutron flux of $\sim 3.3\times10^{7}$ n/s/cm^2 was followed by a 23-day decay period. The multi-parameter FIPPS setup, providing data from 64 detector channels, enabled detailed reconstruction of the entire fission process from irradiation to decay.

Our analysis framework combined machine learning-based spectral analysis with γ-emission simulations, establishing new benchmarks for fission yield measurements. The approach demonstrates the strength of integrating high-precision γ-spectroscopy with advanced computational methods. Cumulative yields for key isotopes were determined with small uncertainties and showed good agreement with evaluated libraries. The developed methodology offers a robust foundation for future fission product studies and nuclear data improvements, applicable to both short- and long-lived isotopes of nuclear relevance.

Keywords: Nuclear Data; Cumulative Fission Yield; FIPPS; Machine Learning Techniques

1. Introduction

Accurate neutron-induced fission yield data are crucial for reactor physics, safeguards, and waste management [1]. Current discrepancies among nuclear databases [2] highlight the need for im-

 ISBN 2654-007X (print), 2654-0088 (online).

proved precision for several isotopes, even for the most commonly used ones [3]. This research focuses on cumulative fission yield measurements using γ-ray spectroscopy, being the first experimental campaign at the Fission Product Prompt γ-ray Spectrometer (FIPPS) [4], exclusively dedicated to this type of measurement. The FIPPS instrument is located at the Institut Laue-Langevin (ILL) [5] in Grenoble, France. This experiment consisted of seven days of continuous irradiation of a ^{235}U target with a thermal neutron beam, followed immediately by a 23-day decay phase [6].

The configuration provided both in-beam and off-beam data, but in this work only the decay-phase data were utilized for the extraction of the cumulative fission yields of several isotopes. The complex configuration of FIPPS setup, delivering data from 64 detector channels, enabled a detailed reconstruction of the entire fission process—from irradiation to decay—through time-resolved γ-ray spectra acquired every five minutes. This high temporal granularity provides significant flexibility for post-processing and spectrum re-creation, allowing analysis of any time interval of the decay stage.

The most challenging part of the analysis was the handling and deconvolution of these complex γ-ray spectra. For this reason, dedicated computational methods were developed specifically for this study to improve spectral fitting, background correction, and isotope identification accuracy.

2. Materials and Methods

2.1 Experimental Setup - The FIPPS Spectrometer

The FIssion Product Prompt-γ-ray Spectrometer (FIPPS) is an instrument for γ-ray spectroscopy of nuclei produced in thermal-neutron–induced reactions, uses a pencil-like, intense thermal neutron beam and an array of HPGe clover detectors. More specifically, the incident neutron beam has a diameter of 15 mm and a flux of 3.3×10^7 neutrons s^{-1} cm^{-2} at the target position. The FIPPS γ-ray detector array, shown schematically in Fig. 1a, is formed by a ring of sixteen HPGe clover detectors, consisting of eight FIPPS and eight IFIN-HH modules. The combined FIPPS+IFIN-HH array (Fig. 1b) covers approximately 70% of the solid angle. Each clover comprises four n-type HPGe crystals, featuring a front-tapered design with a diameter of 50 mm and a length of 80 mm.

Additionally, Anti-Compton Shields (ACS) were only coupled with the FIPPS HPGe detectors to significantly enhance γ-ray background rejection and enhance the peak-to-total ratio, by approximately 70%. These FIPPS HPGe shields, made of BGO crystal, are segmented into three parts: front, back, and side.

2.2 Computational Methods for Isotopic Yield Extraction

Because of a malfunction in data sorting only the data from the 14 best-performing HPGe crystals from the IFIN-HH Clover detectors were used in the final analysis. The yield extraction process requires precise integration of the selected photopeak, with careful consideration of background subtraction, detector efficiency corrections, and decay-time normalization. Equally important is the identification of the optimal time interval for integration, in order to minimize interference from other isotopes. The accurate extraction of isotopic yields from the decay experimental spectra was a significant challenge in this analysis, with two main difficulties emerging:

- Temporal evolution is different among isotopes, making optimal histogram selection non-trivial.
- Potential accuracy loss in conventional peak analysis methods due to manual peak identification.

To systematically address these challenges for dozens of isotopes –each exhibiting multiple γ-ray peaks –an automated analysis pipeline based on machine learning was developed, entirely implemented in Python. The framework includes two complementary components:

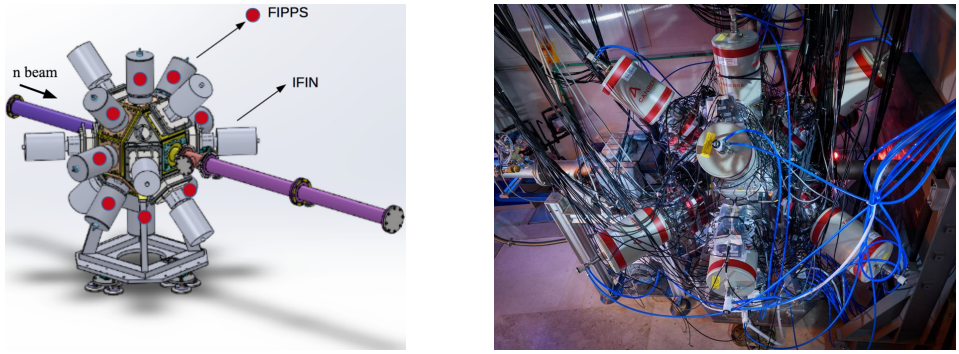

Figure 1. Illustration of the HPGe FIPPS+IFIN-HH detector array. The eight FIPPS clovers, forming a ring around the target position, are highlighted in red. Additionally, four IFIN clovers are positioned on each side of the FIPPS ring. The neutron beam direction is indicated by the beam tubes, shown in purple [7].

1. Neural Network for automated temporal evolution tracking, peak identification, and fitting.
2. Model for the expected γ-ray spectrum for each day of decay, to estimate the optimal time interval for integration.

This integrated approach enhances both the accuracy and efficiency of fission yield determinations compared to conventional analysis methods.

2.2.1 Machine Learning Approach for Peak Extraction

The machine learning approach based on a Neural Network (NN) was developed for the pattern recognition and extraction of the γ-ray peaks from experimental spectra.

The NN architecture processes normalized histograms of γ-ray counts versus energy, where each bin represents the probability density of emissions at that energy. The method generalizes to other isotopes through:

- Pattern recognition of Gaussian-shaped peaks,
- Learning of decay-time correlations, and
- Background continuum estimation.

Generation of Synthetic Spectra

During the learning process, randomly generated peaks are used to build robust feature recognition. The core model relies on constructing a probability density function (PDF) of the form:

$$f(x) = \sum_{i=1} \mathcal{N}(\mu_i, \sigma_i) \cdot I_i \tag{1}$$

subject to the normalization condition:

$$\sum_{i=1} I_i = 1, \qquad \int f(x)\, dx = 1, \tag{2}$$

where each component $\mathcal{N}(\mu_i, \sigma_i)$ represents a normalized Gaussian distribution with intensity I_i, mean μ_i, and standard deviation σ_i. The intensities are constrained such that $\sum_i I_i = 1$, ensuring global normalization.

The NN follows a structured five-step pipeline:

1. **Parameter Sampling:**
   Parameters $\{\mu_i, \sigma_i, I_i\}$:μ_i centered on the desired γ-ray peak energy, fixed σ_i (fixed FWHM) and I_i following a Uniform distribution.
2. **Monte Carlo Generation:**
   For each parameter set, we simulate $N_{\text{events}} = 10^6$ counts distributed according to $f(x)$, incorporating Poisson noise, and flat background (10–20% of total counts).
3. **Histogram Construction:**
   Synthetic spectra are produced from Gaussian distributions with fixed mean energies and sampled intensities. After normalization these histograms are used as input for training the neural network. This step is repeated M times to improve model performance.
   At this stage, we have M different histograms generated from M different parameters set.
4. **NN Method:**
   - **Architecture:** The NN model, built in `TensorFlow/Keras` [8], performs the fitting of each histogram consisting of two hidden layers with a total of 64 neurons, using ReLU activation functions. Batch normalization and a dropout rate of 20% are incorporated to stabilize the training process and reduce overfitting, enabling a reliable extraction of the coefficients f_i.
   - **Training Procedure:** The training is performed using the Adam optimizer ($\eta = 10^{-3}$) together with an early-stopping criterion (patience of 10 epochs), to prevent overfitting. The loss function combines multiple components: $L = \text{MSE} + \lambda \ \|\theta\|_2^2 + \text{MAE}$ [1].
   - **Performance Evaluation:** A total of M=10^6 synthetic spectra are generated for training, partitioned into 70% training, 20% testing, and 10% validation subsets. Additionally, a reduced χ^2 test evaluates the fit quality.

To resume, the NN takes as input an normalized histogram, that derives from experimental spectra, and predicts the f_i components of the histogram, finally succeeding in the identification of γ-ray peaks and extraction of their mean energy, intensity and total integral (Fig. 2).

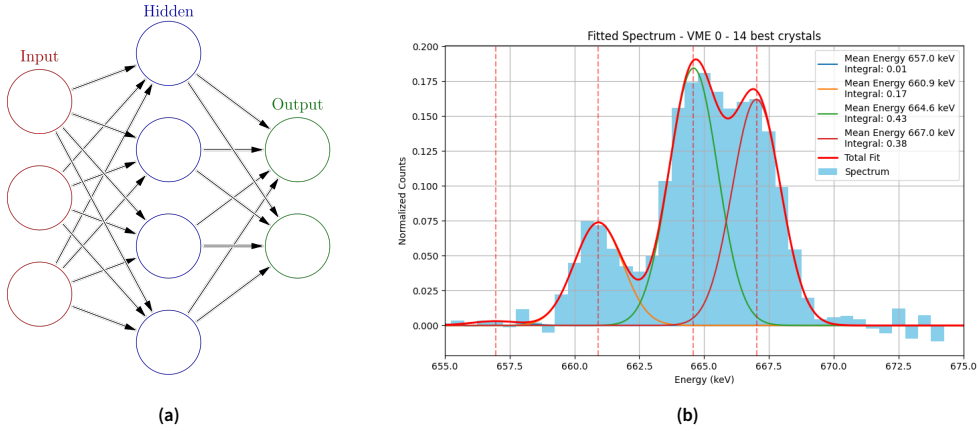

Figure 2. Neural Network analysis approach: (a) Sample architecture of the NN, where the hidden layers perform nonlinear transformations to learn relationships between input features [9]. (b) Fitted spectrum with the NN.

It is important to note that the computational cost of the proposed approach is dominated by the synthetic data generation and the training of the neural network, while the cost associated with

[1] MSE = Mean Squared Error; MAE = Mean Absolute Error

validation and final peak recognition is negligible in comparison. Consequently, the overall computational cost does not depend on the specific input spectrum provided.

For a representative model configuration using approximately 30 bins/keV, four peak mean energies with four corresponding intensities, and a fixed full width at half maximum (FWHM), the total training cost associated with backpropagation (including both forward and backward passes) is estimated to be on the order of 10^9 floating-point operations (FLOPs) per training epoch, corresponding to approximately 10^{-3} TFLOPs per epoch.

On a typical CPU-based system, this complete computational pipeline—including synthetic dataset generation and neural network training—requires approximately 20 min, with synthetic data generation consuming majority of the runtime. Further optimizations, such as accelerated data generation, GPU-based training, and architectural refinements, could significantly reduce the computational time and enable the development of more complex neural network models; however, the present results are obtained using this fully functional neural network configuration.

This machine learning tool was benchmarked against three classical extraction methods: (i) `Cubix`, a ROOT-based automatic peak-fitting routine [10]; (ii) a non-linear least-squares algorithm in Python; and (iii) a ROOT macro developed for this work. The two methods developed in the contect of this work and the respective results are described below:

(ii) The automatic Python least-square fit method fits Gaussian peaks using `scipy.optimize.curve_fit` [11], evaluates the fit via reduced chi-square (χ^2_ν) and p-value, and integrates each peak over $\pm 3\sigma$. Outputs include the background-corrected spectrum, composite fit, and individual components.

(iii) The ROOT macro fits selected histogram regions with three Gaussian and a linear background, computes integrals analytically and numerically, and produces background-subtracted spectra.

Table 1. Comparison of ^{132}I yield results obtained with different methods.

Method	^{132}I	Stat. Uncertainty	p-value
Cubix Integration	32496	± 609	$p \geq 0.05\%$
Python Least-Square fit	32390	± 615	$p \geq 0.05\%$
Neural Network (NN)	32287	± 576	
ROOT Macro Fit	32351	± 561	$p \geq 0.05\%$

According to Table 1 yields were extracted with all four methods (`Cubix`, least-squares, NN, ROOT) and are in agreement within uncertainties for most isotopes. The reason that the value derived by the Neural Network does not come with a p-value is because the NN utilises χ^2 test to do the best fitting of random gaussians during the learning process, but the final result is not a fit. The Neural Network yield extraction method was adopted for the final analysis due to its automation and proved reliability.

2.2.2 Modeling of Gamma Emission Spectra from Fission Products

In this section the computational framework developed to retrieve, process, and model γ-ray emission spectra from fission products for post-irradiation analysis is described.

The mathematical model was based on the Bateman Equations and the decay data were acquired via the IAEA LiveChart API [12]. A ranking function was utilised to identify the most active contributors at each decay time interval. For these isotopes, γ-ray emission histograms were constructed, weighted by activity and intensity. The objective was not to reproduce the experimental spectrum quantitatively, but to develop a representative spectral model that allows the identification of individual γ-ray peaks to their corresponding isotopes, as shown in Fig. 3.

The experimental spectra of Fig. 4 confirm the computational model, showing the same isotopic composition over time. This model assisted in the identification of the optimal γ peaks from the experimental spectra only for quantitative analysis. Thus, cumulative fission product yields were derived by integrating the most prominent, well-separated peaks, reducing the uncertainty. This methodology facilitates both verification of theoretical models and refinement of experimental interpretations through time-dependent spectral analysis.

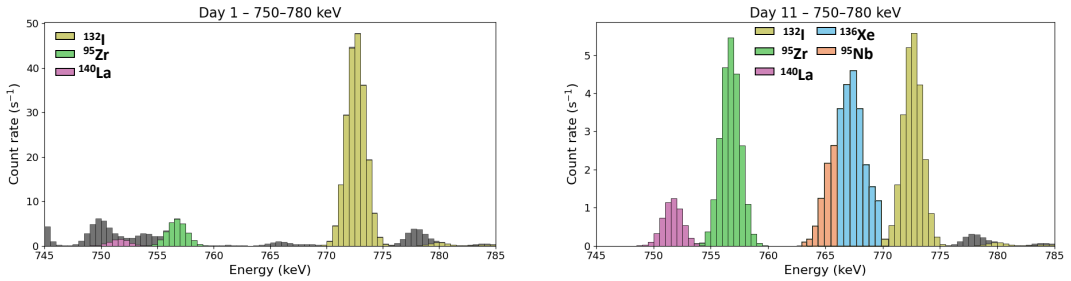

(a) Day 1 post-irradiation, γ-ray spectrum computational prediction

(b) Day 11 post-irradiation, γ-ray spectrum computational prediction

Figure 3. Computation Model using IAEA LiveChart API for fission product decay gamma spectrum prediction in the 745–785 keV energy range.

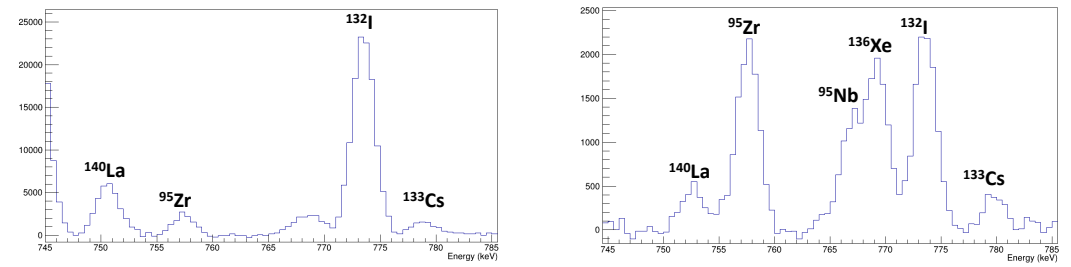

(a) Day 1 post-irradiation data

(b) Day 11 post-irradiation data

Figure 4. Comparison of experimental γ-ray spectra at two different decay stages. (a) Spectrum measured on Day 1 post-irradiation in the 745–785 keV energy range, dominated by contributions from short-lived isotopes. (b) Spectrum measured on Day 11 post-irradiation in the same energy range, dominated by contributions from isotopes with longer half-lives.

It is worth noting that the count rate differs by a factor of 10 between Day 1 and Day 11, as shown in Fig. 4, that is in excellent agreement with the prediction of the computational model, as shown in Fig. 3. Diving more in the details of the experimental spectra, in the spectrum of Day 1 (Fig. 4a), the γ peak at 772.6 keV of ^{132}I, with $t_{1/2} = 2.295$ h, is well resolved due to reduced peak density of the spectral area. On the contrary, in spectrum of Day 11 data (Fig. 4b), the same energy γ peak is partially obscured by the nearby ^{95}Nb, ^{136}Xe and ^{133}Cs γ peaks. In the same spectra, at Day 1 the γ peak at 756.7 keV of ^{95}Zr, with $t_{1/2} = 64.032$ d, is not yet well formed, due to its life-time, while at Day 11 spectrum the γ peak is formed but also is clearly distinct. This is exactly the same patern that was predicted by the computational model, as evident in Fig. 3.

The fact that in specific time integrals the peaks are clearly distinguishable, while in others not, allows their yields to be extracted with significantly lower uncertainty only when the optimal decay stage is chosen. Since the configuration of FIPPS [4] enable detailed reconstruction of each decay stage, simultaneously the challenge of selecting the optimal time interval for each isotope to achieve

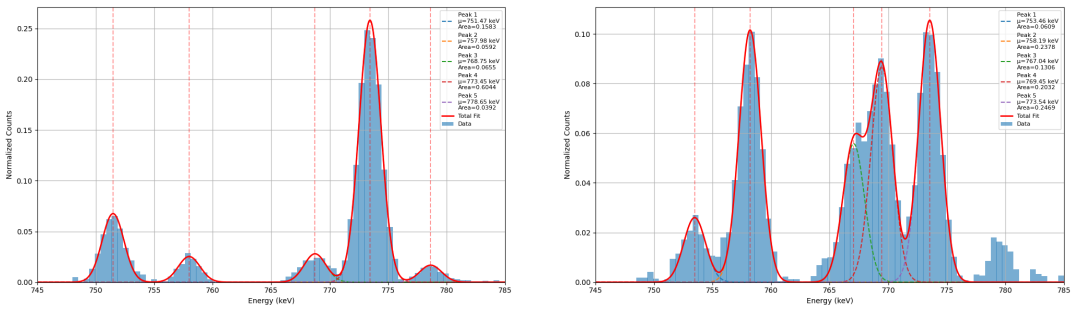

(a) Day 1 post-irradiation, NN

(b) Day 11 post-irradiation, NN

Figure 5. The NN reproduces the main peak positions and relative intensities in the 745–785 keV energy range.

accurate yield determination arises and this model contributes to this crucial selection. The predictive capability of the computational framework is further validated by the NN, which successfully reproduces the main γ-peak positions and relative intensities observed experimentally, as shown in Fig. 5. By coupling the computational predictions for the optimal decay stage with the NN, it becomes possible to move from qualitative spectral identification to quantitative yield extraction with reduced uncertainty. Adopting this robust methodology, the identification and analysis for other nuclei is still ongoing.

3. Results and Discussion

Table 2 presents the nuclear data for the fission products of the heavy mass region. These nuclei are the ones which are identified in the 23-day decay experimental, but also in the γ-emission spectra simulation (§2.2.2). The analysis procedure is still ongoing, so more nuclei utilised for nuclear applications, especially from the light mass region will be published in the future.

Table 2. Cumulative yield results for selected important isotopes including IAEA data from IAEA online repository Live Chart of Nuclides (latest ENSDF file), Y_c with associated statistical and systematic uncertainties from this work, JEFF-4.0 cumulative yields with associated uncertainties, and the percentage difference between the mean values Y_c.

Nuclide	$T_{1/2}$ (s)	E_γ^{IAEA} (keV)	I_γ (%)	Y_c (this work) $\pm\sigma$	Y_c (JEFF- 4.0) $\pm\sigma$	Diff (%)
^{131}I	$6.93 \times 10^5(52)$	364.489(5)	81.5(8)	$(2.96 \pm 0.18) \times 10^{-2}$	$(2.97 \pm 0.14) \times 10^{-2}$	0.47
^{132}Te	$2.77 \times 10^5(1123)$	228.16(6)	88.0(4)	$(3.75 \pm 0.34) \times 10^{-2}$	$(4.26 \pm 0.14) \times 10^{-2}$	5.87
				$(4.01 \pm 0.19) \times 10^{-2}$		
^{132}I	8262(47)	522.65(9)	16.0(5)	$(4.33 \pm 0.18) \times 10^{-2}$	$(4.29 \pm 0.14) \times 10^{-2}$	0.93
		630.19(2)	13.3(4)	$(4.48 \pm 0.34) \times 10^{-2}$		
		667.714(2)	98.7	$(4.67 \pm 0.37) \times 10^{-2}$		
		772.6(1)	75.6(13)	$(4.36 \pm 0.10) \times 10^{-2}$		
		954.55(9)	17.6(5)	$(4.63 \pm 0.16) \times 10^{-2}$		
^{133}I	$7.50 \times 10^4(288)$	529.872(3)	87.0(23)	$(6.64 \pm 0.55) \times 10^{-2}$	$(6.61 \pm 1.32) \times 10^{-2}$	0.45
				$(5.94 \pm 0.31) \times 10^{-2}$		
^{140}Ba	$1.10 \times 10^6(346)$	162.66(1)	6.22(9)	$(6.07 \pm 0.88) \times 10^{-2}$	$(6.16 \pm 0.14) \times 10^{-2}$	1.45
		537.261(9)	24.39(22)	$(5.90 \pm 0.18) \times 10^{-2}$		
^{140}La	$1.45 \times 10^5(18)$	328.762(8)	20.3(3)	$(6.07 \pm 0.20) \times 10^{-2}$	$(6.17 \pm 0.32) \times 10^{-2}$	1.45
		487.021(12)	45.5(6)	$(6.04 \pm 0.21) \times 10^{-2}$		
		815.772(19)	23.28(19)	$(6.09 \pm 0.20) \times 10^{-2}$		
		925.189(21)	6.9(7)	$(5.83 \pm 0.45) \times 10^{-2}$		
		1596.21(4)	95.4(8)	$(6.17 \pm 0.47) \times 10^{-2}$		
^{141}Ce	$2.81 \times 10^6(1123)$	145.4433(14)	48.3(3)	$(6.13 \pm 0.14) \times 10^{-2}$	$(5.97 \pm 0.15) \times 10^{-2}$	2.67
^{143}Ce	$1.19 \times 10^5(22)$	293.266(2)	42.8(4)	$(5.68 \pm 0.61) \times 10^{-2}$	$(5.94 \pm 0.12) \times 10^{-2}$	4.39

The validation of experimental fission yields against nuclear data libraries serves as a crucial benchmark for both theoretical models and experimental methodologies. That is the reason why in the same Table 2 the comparison with the JEFF-4.0 [13] library is presented. This latest release is chosen as it incorporates substantial improvements in fission product yields and their covariance matrices.

4. Conclusions

This fission yield campaign using the Fission Product Prompt γ-ray Spectrometer (FIPPS) at ILL successfully demonstrated the capability for $^{235}\mathrm{U}(n_{\mathrm{th}}, f)$ investigations and highlighted key areas for improvement in the facility.

The combined use of machine learning and physics-based simulations established a powerful computational framework for the extraction and interpretation of γ-ray spectra from fission products. The Neural Network model, trained on a large set of synthetic spectra, demonstrated strong capabilities in automated peak identification, background estimation, and temporal evolution tracking, substantially reducing human bias and improving the precision of yield determination compared to conventional methods. In parallel, the model of γ-ray spectra time evolution guided the optimal selection of integration intervals. Together, these complementary approaches provided a consistent, data-driven and physically grounded analysis framework that enhances both accuracy and reproducibility in fission yield evaluations.

Future work will focus on refining decay stage selection, improving counting statistics, and minimizing spectral interferences to further reduce uncertainties across the full mass-yield distribution.

Funding statement

This work was supported by the poject “SINET” of CEA, the ERASMUS+ mobility Program [14] and the ENEN2plus Project [15]. The authors are grateful for the support of ILL and all the staff involved from CEA, NTUA and LPSC.

References

[1] V. Vallet, A. Rizzo, M. Tiphine, and T. Nicol. “Data assimilation of decay heat experiments for feedback on nuclear data”. In: *EPJ N* 10 (2024), p. 11. DOI: 10.1051/epjn/2024011.
[2] F. P. An et al. “Comprehensive Measurement of the Reactor Antineutrino Spectrum and Flux at Daya Bay”. In: *Phys. Rev. Lett.* 134 (2025), p. 201802. DOI: 10.1103/PhysRevLett.134.201802.
[3] L. A. Bernstein, D. A. Brown, A. J. Koning, B. T. Rearden, C. E. Romano, A. A. Sonzogni, A. S. Voyles, and W. Younes. “Our Future Nuclear Data Needs”. In: *Ann. Rev. Nucl. Part. Sci.* 69 (2019), pp. 109–136. ISSN: 1545-4134. DOI: 10.1146/annurev-nucl-101918-023708.
[4] C. Michelagnoli et al. *FIPPS (FIssion Product Prompt γ-ray Spectrometer) and its first experimental campaign*. 2018. DOI: 10.1051/epjconf/201819304009.
[5] Institut Laue-Langevin (ILL). https://www.ill.eu/about-the-ill/ill-at-a-glance.
[6] O. Serot et al. *Accurate measurements of cumulative fission product yields from* $^{235}\mathrm{U}(\mathrm{n_{th}}, \mathrm{f})$. ILL Experiment Report. 2024. DOI: 10.5291/ILL-DATA.3-17-74.
[7] *The FIPPS Instrument*. https://www.ill.eu/for-ill-users/instruments/instruments-list/fipps/description/fipps-ifin.
[8] M. Abadi et al. *TensorFlow: Large-Scale Machine Learning on Heterogeneous Systems*. Software available from tensorflow.org. 2015. URL: https://www.tensorflow.org/.
[9] https://en.wikipedia.org/wiki/Neural_network_(machine_learning).
[10] J. Dudouet. *Cubix*. https://zenodo.org/records/15602270. 2024.
[11] P. Virtanen et al. *SciPy 1.0: Fundamental Algorithms for Scientific Computing in Python*. 2020. DOI: 10.1038/s41592-019-0686-2.
[12] IAEA Nuclear Data Section. *Livechart Data Download API*. https://www-nds.iaea.org/relnsd/vcharthtml/api_v0_guide.html.
[13] Joint Evaluated Fission and Fusion Project. *JEFF-4.0 Evaluated Data: neutron data [Data set]. OECD Nuclear Energy Agency*. EPJ N vol. 10. 2025. DOI: 10.82555/e9ajn-a3p20.
[14] *ERASMUS+ Programme*. https://erasmus-plus.ec.europa.eu/.
[15] *ENEN2plus project*. https://enen.eu/index.php/portfolio/enen2plus-project/. 2024.